Image simulation of a laser-illuminated scattering layer in turbulent atmosphere

V.A. Banakh

Institute of Atmospheric Optics,
Siberian Branch of the Russian Academy of Sciences, Tomsk

Image simulating algorithms for a laser-illuminated scattering layer in turbulent atmosphere are presented. The examples of using these algorithms to proof the speckle photography usability for visualization of enhanced turbulence zones in the atmosphere are cited.

When developing the speckle-photography[3] rendering methods for searching and visualization of zones of enhanced atmospheric turbulence,[1,2] the need in detailed analysis of capabilities and accuracy of these methods under different atmospheric conditions is of importance. Such analysis is impossible without modern computer technologies. However, direct simulation of laser radiation propagation along paths with reflection in turbulent atmosphere through imaging a laser-illuminated area of the scattering surface requires so large working memory and time consumption, that becomes impossible when using standard personal computers.

The problem of imaging the illumination spot of the scattering atmospheric layer is formulated in this work and possible ways of its numerical solution for some special cases are described.
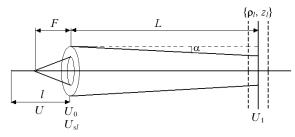
Consider an optical diagram (Fig. 1).

Fig. 1. The diagram of laser radiation propagation.

A laser pulse with the initial distribution $U_0(0, \rho', t)$ passes the distance L in the atmosphere and then scatters on some atmospheric layer. The scattered radiation is received by a telescope with a photodetector array in the receiving plane. The complex amplitude of the scattering-particle incident field is written as

$$U_1(z_l, \rho_l, t) = K^{1/2}(z_l)\frac{k e^{ikz_l}}{2\pi i z_l} \int d^2\rho'\, U_0\left(\rho', t - \frac{z_l}{c}\right) \times$$

$$\times \exp\left\{\psi(\rho', \rho_l) + i\frac{k}{2z_l}(\rho_l - \rho')^2\right\}, \qquad (1)$$

where z_l is the longitudinal coordinate of the scattering particle; ρ_l is the radius-vector determining the particle position in the transversal plane; c is the light speed; t is the time; $\psi = \chi + iS$, χ is the amplitude noise and S is the phase jitter of a partial spherical wave propagating from $(0, \rho')$ plane to the (z_l, ρ_l) point; $K(z_l)$ is the attenuation function; $k = 2\pi/\lambda$ is the wave number; i is the imaginary unit.

The complex amplitude of the field scattered by the particle in the plane $z = 0$ is written as

$$U_{sl}(0, \rho'', t) = \frac{\alpha_l e^{ikz_l}}{z_l} K^{1/2}(z_l) U_1\left(z_l, \rho_l; t - \frac{z_l}{c}\right) \times$$

$$\times \exp\left\{\psi(\rho_l, \rho'') + i\frac{k}{2z_l}(\rho'' - \rho_l)^2\right\}, \qquad (2)$$

where α_l is the particle scattering amplitude; $\psi(\rho_l, \rho'')$ is the random complex phase incursion of a spherical wave propagating back from the particle to telescope.

The integrated field in the $(0, \rho'')$ plane is defined as a sum of the right part of Eq. (2) over all scattering particles N_s in the layer

$$U_s = \sum_{l=1}^{N_s} U_{sl}.$$

For the thin scattering layer $|z_l - L| \ll L$, we can assume $t = 2L/c$, $z_l \approx L$ in Eq. (2), leaving the z_l-dependence only in the fast oscillating multiplier e^{ikz_l}.

Finally, for the field in the telescope receiving plane (l, ρ) we obtain

$$U(l, \rho, t) = \frac{k}{2\pi i l}\exp\left\{ikl + ik\frac{\rho^2}{2l}\right\} \times$$

$$\times \int d\rho''\, T(\rho'') U_s\left(0, \rho'', \frac{2L}{c}\right)\left\{-i\frac{k}{l}\rho\rho'' + ik\left(\frac{1}{l} - \frac{1}{F}\right)\rho''^2\right\}, \quad (3)$$

where $T(\rho'')$ is the amplitude transmission factor of the receiving aperture; F is the telescope focal length.

As it follows from Eq. (3), the received radiation strength in the $(l, \boldsymbol{\rho})$ plane

$$I(l, \boldsymbol{\rho}, t) = |U(l, \boldsymbol{\rho}, t)|^2 \tag{4}$$

is defined by the equation

$$I(l,\boldsymbol{\rho},t) = \left(\frac{k}{2\pi l}\right)^2 \left| \int d\boldsymbol{\rho}'' T(\boldsymbol{\rho}'') U_s\left(0,\boldsymbol{\rho}'',\frac{2L}{c}\right) \times \right.$$

$$\left. \times \left\{ -i\frac{k}{l}\boldsymbol{\rho}\boldsymbol{\rho}'' + ik\left(\frac{1}{l} - \frac{1}{F}\right)\boldsymbol{\rho}''^2 \right\} \right|^2. \tag{5}$$

Introduce the parabolic equation Green functions for the complex field amplitude in the direct and backward direction as applied to the propagation geometry in Fig. 1:

$$G(0,\boldsymbol{\rho}';L,\boldsymbol{\rho}_l) = \frac{K^{1/2}(L)e^{ikz_l}}{2\pi iL} \times$$

$$\times \exp\left\{ \psi(\boldsymbol{\rho}',\boldsymbol{\rho}_l) + i\frac{k}{2L}(\boldsymbol{\rho}_l - \boldsymbol{\rho}')^2 \right\}, \tag{6a}$$

$$G(L,\boldsymbol{\rho}_l;0,\boldsymbol{\rho}'') = \frac{K^{1/2}(L)e^{ikz_l}}{2\pi iL} \times$$

$$\times \exp\left\{ \psi(\boldsymbol{\rho}_l,\boldsymbol{\rho}'') + i\frac{k}{2L}(\boldsymbol{\rho}'' - \boldsymbol{\rho}_l)^2 \right\}. \tag{6b}$$

Using Eqs. (6a) and (6b), for the field U_s in Eq. (5) obtain

$$U_s\left(0,\boldsymbol{\rho}'',\frac{2L}{c}\right) = \frac{2\pi i}{k} \sum_{l=1}^{N_s} \alpha_l \, G(L,\boldsymbol{\rho}_l;0,\boldsymbol{\rho}'') \times$$

$$\times \int d\boldsymbol{\rho}' U_0\left(\boldsymbol{\rho}',\frac{2}{c}(L - z_l)\right) G(0,\boldsymbol{\rho}';L,\boldsymbol{\rho}_l) =$$

$$= \frac{2\pi i}{k} \sum_{l=1}^{N_s} \alpha_l \, G(L,\boldsymbol{\rho}_l;0,\boldsymbol{\rho}'') U_1\left(L,\boldsymbol{\rho}_l;\frac{2}{c}(L - z_l)\right), \tag{7}$$

which allows Eq. (5) to be presented in the form

$$I(l,\boldsymbol{\rho},t) = \frac{1}{l^2} \sum_{l=1}^{N_s} \sum_{l'=1}^{N_s} \alpha_l \alpha_{l'} \int d\boldsymbol{\rho}_{1,2} T(\boldsymbol{\rho}_1) T^*(\boldsymbol{\rho}_2);$$

$$G(L,\boldsymbol{\rho}_l;0,\boldsymbol{\rho}_1) G^*(L,\boldsymbol{\rho}_{l'};0,\boldsymbol{\rho}_2) \times$$

$$\times U_1\left(L,\boldsymbol{\rho}_l;\frac{2}{c}(L - z_l)\right) U_1^*\left(L,\boldsymbol{\rho}_{l'};\frac{2}{c}(L - z_{l'})\right) \times$$

$$\times \exp\left\{ -i\frac{k}{l}\boldsymbol{\rho}(\boldsymbol{\rho}_1 - \boldsymbol{\rho}_2) + ik\left(\frac{1}{l} - \frac{1}{F}\right)(\boldsymbol{\rho}_1^2 - \boldsymbol{\rho}_2^2) \right\}. \tag{8}$$

Items with $l \neq l'$ in Eq. (8) can be ignored in the case of arbitrary stochastic distribution of initial space positions of scattered particles due to the fast oscillating multipliers e^{ikz_l}, if the scale of probability distribution function variations significantly exceeds the wavelength of the scattered field.[4] The scales of turbulent inhomogeneities of the atmospheric velocity field essentially exceeds the length of optical waves, hence, we can use this approximation and restrict ourselves to the items with $l \neq l'$ in Eq. (8). As a result, obtain

$$I(l,\boldsymbol{\rho},t) = \frac{1}{l^2} \sum_{l=1}^{N_s} |\alpha_l|^2 \int d\boldsymbol{\rho}_{1,2} T(\boldsymbol{\rho}_1) T^*(\boldsymbol{\rho}_2) \times$$

$$\times G(L,\boldsymbol{\rho}_l;0,\boldsymbol{\rho}_1) G^*(L,\boldsymbol{\rho}_l;0,\boldsymbol{\rho}_2) \times$$

$$\times U_1\left(L,\boldsymbol{\rho}_l;\frac{2}{c}(L - z_l)\right) U_1^*\left(L,\boldsymbol{\rho}_l;\frac{2}{c}(L - z_l)\right) \times$$

$$\times \exp\left\{ -i\frac{k}{l}\boldsymbol{\rho}(\boldsymbol{\rho}_1 - \boldsymbol{\rho}_2) + ik\left(\frac{1}{l} - \frac{1}{F}\right)(\boldsymbol{\rho}_1^2 - \boldsymbol{\rho}_2^2) \right\}. \tag{9}$$

Replace the summation in Eq. (9) by the scattering volume integration

$$\sum_{i=1}^{N_s} \to \int_{-\infty}^{\infty} dz_l \int_{-\infty}^{\infty} d\boldsymbol{\rho}_l,$$

introduce the average backscatter cross section $<|\alpha_l|^2> = \theta_s$ and the concentration of the scattering particles ρ_s. Then, for Eq. (9) will be

$$I(l,\boldsymbol{\rho},t) = \frac{\rho_s \theta_s}{l^2} \int_{-\infty}^{\infty} dz_l \int_{-\infty}^{\infty} d\boldsymbol{\rho}_l \, I_1\left(L,\boldsymbol{\rho}_l;\frac{2}{c}(L - z_l)\right) \times$$

$$\times \left| \int d\boldsymbol{\rho}'' T(\boldsymbol{\rho}'') G(L,\boldsymbol{\rho}_l;0,\boldsymbol{\rho}'') \exp\left\{ -i\frac{k}{l}\boldsymbol{\rho}\boldsymbol{\rho}'' + ik\left(\frac{1}{l} - \frac{1}{F}\right)\boldsymbol{\rho}''^2 \right\} \right|^2, \tag{10}$$

where

$$I_1 = |U_1|^2;$$

$$U_1 = \int d\boldsymbol{\rho}' U_0\left(\boldsymbol{\rho}',\frac{2}{c}(L - z_l)\right) G(0,\boldsymbol{\rho}';L,\boldsymbol{\rho}_l)$$

and the Green functions do not contain multipliers e^{ikz_l}.

Let us integrate over the longitudinal coordinate z_l in Eq. (10) using the Gaussian model for initial field distribution:

$$U_0(\boldsymbol{\rho}',t) = \frac{P^{1/2}(t)}{\sqrt{\pi}a} \exp\left\{ -\frac{\boldsymbol{\rho}'^2}{2a^2} - i\frac{k}{2f}\boldsymbol{\rho}'^2 \right\}, \tag{11}$$

where

$$P(t) = \frac{U_p}{\sqrt{\pi}\sigma} e^{-t^2/\sigma^2}; \quad \int_{-\infty}^{+\infty} dt \int_{-\infty}^{+\infty} d^2\boldsymbol{\rho}' \left|U_0(\boldsymbol{\rho}',t)\right|^2 = U_p;$$

σ determines the pulse duration; a and f are the beam radius and the radius of phase front curvature, respectively:

$$\frac{U_p}{\sqrt{\pi}\sigma} \int_{-\infty}^{+\infty} dz_l \exp\left\{ -\frac{4}{c^2}\frac{(L - z_l)^2}{\sigma^2} \right\} = \frac{U_p c}{2}. \tag{12}$$

Finally, for the intensity distribution in the image of laser-illuminated atmospheric layer, obtain

$$I(l,\rho,L,t) = \frac{\beta\pi}{l^2}\frac{U_p c}{2}\int d\rho_l\, I_1(L,\rho_l)I_t(L,\rho_l,\rho), \quad (13)$$

where

$$I_1(L,\rho_l) = \left|\int d\rho' \exp\left\{-\frac{\rho'^2}{2a^2}(1+ika\alpha)\right\}G(0,\rho';L,\rho_l)\right|^2, (14)$$

$$I_t(L,\rho_l,\rho) = \left|\int d\rho''\, T(\rho'')\times\right.$$

$$\left.\times \exp\left\{-i\frac{k}{l}\rho\rho'' + ik\left(\frac{1}{l}-\frac{1}{F}\right)\rho''^2\right\}G(0,\rho'';L,\rho_l)\right|^2; \quad (15)$$

$\beta\pi = \rho_s\theta_s$ designates the backscattering coefficient and $\alpha = a/f$ defines the initial beam divergence. In accordance with the reciprocity theorem,[5,6] the Green function for the backward propagation in Eq. (13) is written in the form corresponding to the forward propagation.

Thus, it follows from Eq. (13) that the intensity of the image of laser-illuminated atmospheric layer is completely determined by the integral of the product intensity distribution on the layer of the illuminating laser beam [Eq. (14)] and the "beam" with parameters of the receiving telescope and propagating forward as well [Eq. (15)]. Equation (13) is correct up to numerical coefficients not only for atmospheric scattering of pulse radiation, but also for continuous radiation reflected from a "hard" diffusive surface.

Equation (13) permits a generalization. In the case of irregular layer concentration of scatterers, Equation (3) takes the form

$$I(l,\rho,L,t) = \frac{\theta_s}{l^2}\frac{U_p c}{2}\int d\rho_l\, \rho_s(\rho_l)I_1(L,\rho_l)I_t(L,\rho_l,\rho), \quad (16)$$

where $\rho_s(\rho_l)$ can be random function in general case. Incomplete spatial coherence of a source can be accounted for via using the following model for the initial field distribution instead of Eq. (11):

$$U_0(\rho',t) = \frac{P^{1/2}(t)}{\sqrt{\pi}a}\exp\left\{-\frac{\rho'^2}{2a^2}-i\frac{k}{2f}\rho'^2\right\}\exp\left\{iS_s(\rho')\right\}=$$

$$= U_{0s}(\rho',t)\exp\left\{iS_s(\rho')\right\}, \quad (17)$$

where the random phase $S_s(\rho')$ is defined by the correlation function

$$\psi_s(\rho') = <S_s(\rho'_1)S_s(\rho'_2+\rho')> = \sigma_s^2 K_s(\rho') \quad (18)$$

with the dispersion σ_s and the spatial correlation coefficient $K_s(\rho')$.

The function of spatial field coherence of a laser source for model (17) is written in the form[7]

$$\Gamma_0(\rho') = <U_0(\rho'_1,t)U_0^*(\rho'_2,t)> =$$

$$= U_{0s}(\rho'_1,t)U_{0s}^*(\rho'_2,t)\exp\left\{\sigma_s^2\left[K_s^2(\rho')-1\right]\right\}. \quad (19)$$

It follows from Eq. (19), that the radius of spatial source coherence $a_k \sim l_s$ is comparable with the scale of phase correlation $l_s \sim |K_s''|^{-1/2}$, while at large phase fluctuations $\sigma_s^2 \gg 1$ the radius of field coherence is defined by the ratio $a_k \sim l_s/\sigma_s$.

Finally, Eq. (13) for scattering particles, changing their positions in space, written for the time moment $t + \Delta t$ has the form

$$I(l,\rho,L,t+\Delta t) = \frac{\beta\pi}{l^2}\frac{U_p c}{2}\times$$

$$\times \int d\rho_l\, I_1\left[L,\rho_l(\Delta t)\right]I_t\left[L,\rho_l(\Delta t),\rho\right], \quad (20)$$

where $\rho_l(\Delta t) = \int\limits_0^{\Delta t}\mathbf{V}\left[\tilde{\rho}_l(\tilde{\rho}_l,\tau)\right]$; $\mathbf{V}(\rho_l)$ is the speed vector of scattering particles migration within the layer, which is normal to the direction of illuminating beam propagation. The speed vector $\mathbf{V}(\rho_l)$ can have a complicated functional dependence on ρ_l and be random.

The algorithm for computing the intensity distribution by Eq. (13) is the following: the forward propagation of two beams to the scattering layer is simulated, e.g., using the splitting technique over physical factors,[8] their intensities are computed, then multiplied, and the result is integrated in general case with the weight function $\rho_s(\rho_l)$. But such direct integration is not always possible due to large time consumption. The simulation problem is essentially simplified at $l = F$, if the turbulence effect is negligible, like, for example, in case of high-altitude propagation path or vertical and slant propagation paths, when the distorting layer is adjacent to a receiver-transmitter and the turbulence effect is well phase screen approximated.[9] Then Equation (13) takes the form of convolution integral

$$I(F,\rho,L,t) \sim \int d\rho_l\, I_1(L,\rho_l)I_t(L,\rho_l-\rho) \quad (21)$$

and the algorithm for imaging the illuminated layer is reduced to the computation of Fourier transform of I in the image as a product of Fourier transforms of the I_1 and I_t:

$$\tilde{I}(F,\kappa,L,t) \sim \tilde{I}_1(L,\kappa)\tilde{I}_t(L,\kappa,\rho),$$

and computation of the inverse Fourier transform

$$I(F_t,\rho) = \int d\kappa\, \tilde{I}_1(L,\kappa)\tilde{I}_t(L,\kappa,\rho)\,e^{i\kappa\rho}. \quad (22)$$

The use of the fast Fourier transform provides for the intensity computation in image at quite acceptable time costs.

Another algorithm is based on the illuminated beam squared intensity approximation:

$$I(F,\boldsymbol{\rho},L,t) \simeq \int d\boldsymbol{\rho}_l\, I_1^2(L,\boldsymbol{\rho}_l) I_t^0(L,\boldsymbol{\rho}_l,\boldsymbol{\rho}), \qquad (23)$$

where $I_t^0(L,\boldsymbol{\rho}_l,\boldsymbol{\rho})$ is the beam intensity distribution with parameters, determined by the parameters of a receiving telescope in the plane of scattering layer, computed for homogeneous medium. According to Eq. (23), "scanning" of the illumination spot is performed with a telescopic beam; turbulent distortions in this case are taken into account under the assumption that they are similar for illuminating and telescopic beams, that is valid when using a narrow-field receiving telescope.
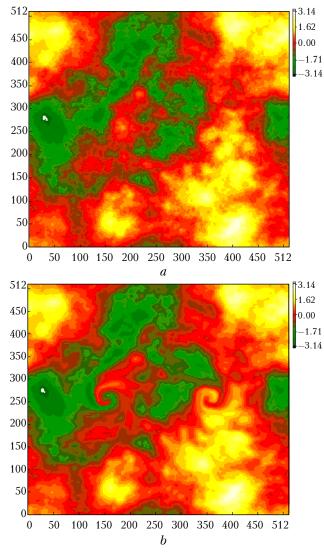
Both algorithms were tested in numerical experiments,[1,2,10,11] in particular, in analyzing the capabilities to visualize eddy regions of the enhanced turbulence in aircraft traces and wind velocity measurements by the speckle photography.[1,2,10] The computer simulation results for the visualization of vortexes followed the aircraft in air[2] are shown in Fig. 2. The intensity distribution in the image of scattering layer computed for the optical diagram (see Fig. 1) by algorithm [Eq. (23)] at the time point t [Eq. (13)] is shown in Fig. 2*a* and at the time point $t + \Delta t$ [Eq. (20)] — in Fig. 2*b*. Changing of positions of scattering particles in the layer $\boldsymbol{\rho}_l(\Delta t)$ was simulated following the model for the tangential velocity in aircraft vortexes.[12] Vortex structures are clearly seen in the image. They arise due to the transfer of scattering particles and turbulent inhomogeneities along the propagation path by the aircraft vortex velocity field.

Acknowledgements

References

1. T. Halldorsson, A. Langmeier, A. Prucklmeier, V.A. Banakh, and A.V. Falits, Proc. SPIE **6522**, 8 (2006).
2. V. Banakh, A. Falits, and T. Halldorsson, in: *Lidar Technologies, Techniques, and Measurements for Atmospheric Remote Sensing II: Abstracts,* Stockholm (2006), p. 100.
3. N.A. Fomin, *Speckle Photography for Fluid Mechanics Measurements* (Springer–Verlag, 1998), 290 pp.
4. B. Crosignani, P. Di Porto, and M. Bertolotti, *Statistical Properties of Scattered Light* (Academic Press, New York – San Francisco – London, 1975), 206 pp.
5. V.I. Gelfgat, Akust. Zh. **22**, Is. 1, 123–124 (1976).
6. V.A. Banakh and V.L. Mironov, *Lidar in a Turbulent Atmosphere* (Artech House, Boston & London, 1987), 185 pp.
7. S.M. Rytov, Yu.A. Kravtsov, and V.I. Tatarskii, *Introduction in Statistical Radiophysics* (Nauka, Moscow, 1978), 463 pp.
8. V.P. Kandidov, Usp. Fiz. Nauk **166**, No. 12, 1309–1338 (1996).
9. V.A. Banakh and I.N. Smalikho, Atmos. Oceanic Opt. **6**, No. 4, 233–237 (1993).
10. V.A. Banakh, A.V. Falits, and T. Halldorsson, in: *Proc. 13th Coherent Laser Radar Conf.* 2005. P. 19–22.
11. V.A. Banakh, D.S. Rytchkov, and A.V. Falits, Proc. SPIE **6160**, 61600Q-1–61600Q-7 (2005).
12. H. Lamb, *Hydrodynamics*. 6th ed. (Dover, New York, 1932), P. 592 [Chapter 11].

Fig. 2. Visualization of aircraft vortex shedding: $L = 1$ km; $C_n^2 = 10^{-15}$ m$^{-2/3}$; $\alpha = 30''$; effective diameter of the telescope aperture is 0.2 m.